



# Reply to the Discussion on “Granite-pegmatite-related gold skarns and associated Li-Cs-Ta pegmatites in the Archean Yilgarn Craton, Western Australia” by Witt (2025)

Andreas G. Mueller<sup>1</sup>

Received: 13 December 2025 / Accepted: 23 December 2025  
© The Author(s) 2026

I welcome the opportunity to clarify the issues raised by Witt (2025) about the relationship of gold skarn deposits and LCT pegmatites to the post-orogenic I-type granite suite in the east-central Yilgarn Craton. As also discussed in Witt et al. (2001), these issues are:

- (1) the interpretation of biotite alteration in the footwall amphibolite of mineralized banded iron-formation at Nevorlia as seafloor and pre-metamorphic;
- (2) uncertainty about the timing of amphibolite-facies metamorphism related to the Ghooli Dome batholith;
- (3) the interpretation of the high-T (650–400°C) gold deposits in the Southern Cross greenstone belt as syn-metamorphic rather than as gold skarns; and
- (4) uncertainties about the spatial, temporal and genetic relationship of the gold deposits to I-type granites and LCT pegmatites.

## Pre-metamorphic seafloor alteration

Witt (2025) re-interprets the replacement in amphibolite at Nevorlia (Mueller 1997) as pre-metamorphic syn-volcanic alteration stratabound to banded iron-formation (BIF). He correlates the exhalative BIF-horizon with pyrrhotite lenses in the Yilgarn Star and Great Victoria gold deposits. Both deposits are bound to the contact with graphitic meta-greywacke, the uppermost stratigraphic unit separated from the BIF by a volcanic succession at least 1 km thick. My mapping has

shown that the Nevorlia Anticline, defined by beds of silicate-facies grunerite-quartz±magnetite iron formation, is refolded around the Ghooli orthogneiss dome (Fig. 1). Gold skarn in BIF and related contact alteration occur at and between the Nevorlia and Kurrajong open pits but do not extend to the entire BIF marker horizon. At Nevorlia, alteration is bound to lithologic contacts in both the hanging wall and footwall of the BIF beds (Fig. 4 in Mueller 2025), and does not display the asymmetric geometry of seafloor hydrothermal systems. Witt (2025; his Fig. 1) describes the footwall replacement in amphibolite as “biotite-cordierite-plagioclase-quartz schist” below a “cumingtonite” bed (=BIF?) but ignores that the plagioclase is anorthite, a common skarn calc-silicate (Meinert et al. 2005). Massive to banded anorthite-rich skarn is widespread in the footwall of Nevorlia gold ore, where it forms equilibrium assemblages with biotite, cumingtonite, and anthophyllite (Figs. 2a–d). Almandine and cordierite are restricted to biotite-rich zones 5–20 cm thick. The other common skarn type is zoned from inner diopside to outer hornblende+pargasite, and then to biotite and Fe-Mg chlorite, where prehnite and/or phengite+zoisite are stable instead of plagioclase (Figs. 2e, f). Clearly, this represents primary metasomatic zonation to outer low-T assemblages (<400 °C; Liou et al. 1983), and not equilibrium at amphibolite-facies conditions. Scheelite-bearing skarn veins (Figs. 2g, h) occur between actinolite-hedenbergite gold skarn in BIF, which also contains scheelite. The carbonate-rich veins and alteration zones inferred as precursor rocks for Witt’s metamorphic model (Witt 2025; his Fig. 1) occur at Nevorlia but are controlled by post-gold brittle faults (Mueller 1997).

Editorial handling: B. Lehmann

✉ Andreas G. Mueller  
andreas.mueller2@partner.kit.edu

<sup>1</sup> Karlsruhe Institute of Technology, Applied Geosciences, Adenauerring 20b, D-76131 Karlsruhe, Germany

## Ghooli dome amphibolite-facies aureole

The Marvel Loch and Nevorlia gold deposits are both located in the km-wide amphibolite-facies aureole bordering the Ghooli Dome orthogneiss batholith (Ahmat 1986).

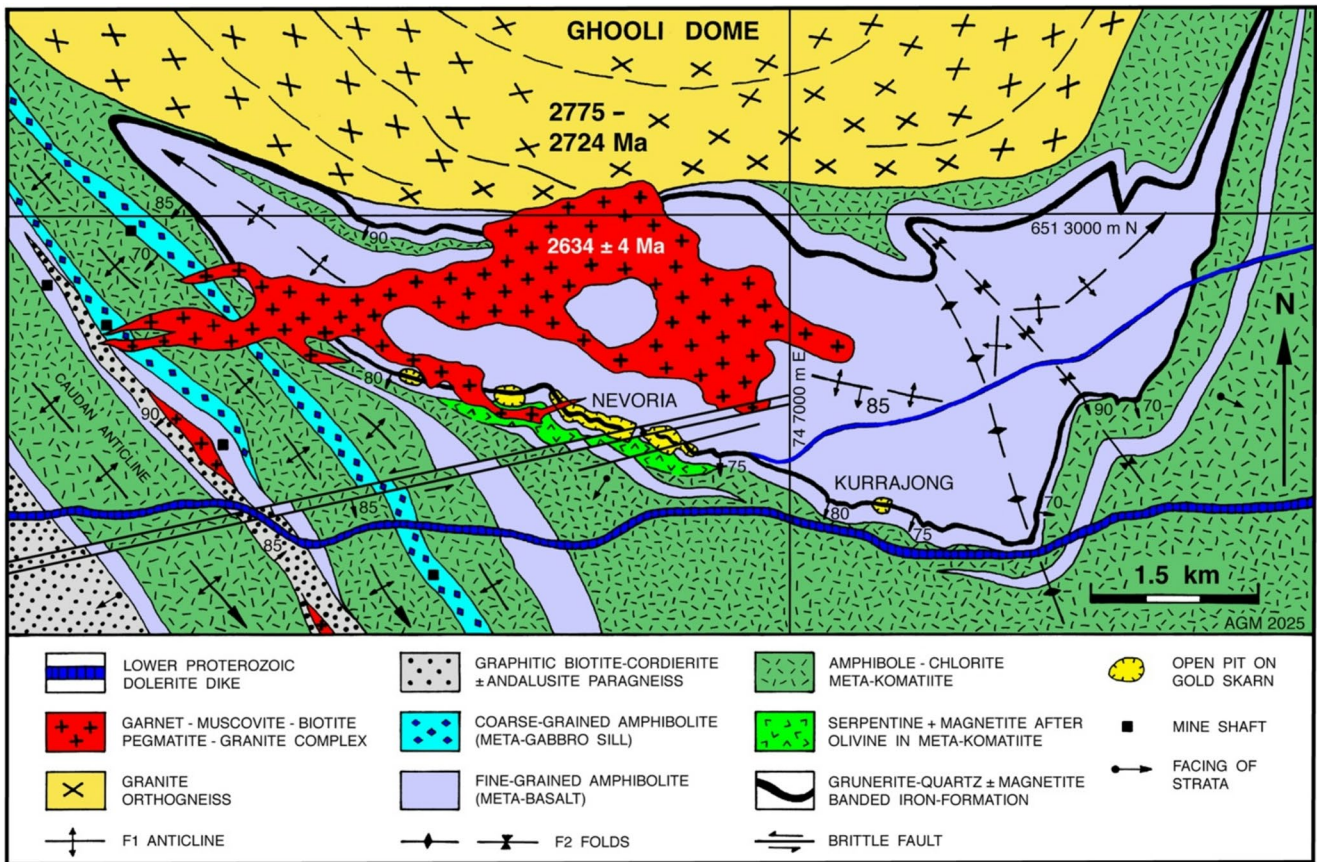


**Fig. 1** Bedrock map of the Nevoria mine area (modified from Mueller et al. 2004) in the 3.0 Ga Southern Cross greenstone belt, Yilgarn Craton. Beds of banded iron-formation (BIF) outline the Nevoria Anticline (F1) refolded around the Ghooli orthogneiss dome. F2 surfaces display a fan-shaped geometry. Gold skarn in grunerite-quartz ± magnetite BIF was mined in the Nevoria and Kurrajong open pits. The

The age of aureole metamorphism in the 3.0 Ga Southern Cross greenstone belt is constrained by metamorphic zircons ( $2772 \pm 5$  Ma) in a 2.91 Ga quartz porphyry sill located adjacent to the border granite gneiss ( $2775 \pm 10$  Ma) of the Ghooli Dome (Mueller and McNaughton 2000). Similar ages ( $2911 \pm 5$  Ma;  $2777 \pm 9$  Ma) were obtained by Lu et al. (2017) in zircons from the same altered porphyry. The U-Pb zircon ages of granitoids in the Ghooli Dome range from 2775–2721 Ma ( $n=4$ ) in the southeast, and from 2720–2691 Ma ( $n=5$ ) in the northwest (Doublie et al. 2014). Enclaves of older orthogneiss (2.93–2.92 Ga) were dated at two localities (Thebaud et al. 2013a, b). Steeply plunging mineral lineations in the greenstone belt, for example in amphibolite between the Nevoria BIFs (Mueller 1997), link aureole metamorphism to the emplacement of the batholith (Dalstra et al. 1998). Most amphibolites and meta-komatiites, however, are massive or foliated rather than lineated (Mueller 1991, 1997), textures incompatible with a 5–6 km rise of the solid-state batholith (Dalstra et al. 1998; Witt 2025). Cataclastic mylonites with shallowly

pegmatite-granite pluton ( $2634 \pm 4$  Ma) north of the mine workings dips 15–20° south, and underlies the Nevoria ore bodies at 200–250 m depth. The gold skarn is dated by an allanite-in-almandine U-Pb age of  $2635.7 \pm 1.2$  Ma (Mueller et al. 2004). The coordinates are Map Grid Australia Zone 50.

plunging lineations caused by strike-slip on the Koolyanobbing Fault cut orthogneiss at the NE-margin of the Ghooli Dome (Libby et al. 1991). They are crosscut by massive biotite granite dated at  $2656 \pm 3$  Ma (Qiu et al. 1999). Clearly, the uplift of the batholith did not continue until 2620 Ma (Witt 2025). At Nevoria, metamorphic temperature is estimated at  $610 \pm 50$  °C (Mueller et al. 2004), a result similar to the fluid temperature of  $590 \pm 50$  °C based on prograde skarn equilibrium assemblages (Figs. 2a-c). However, geothermometers do not measure time. The Nevoria gold skarn has been dated by a concordant allanite-in-almandine U-Pb age at  $2635.7 \pm 1.2$  Ma (Mueller et al. 2004). Skarn formation at Nevoria thus postdates granitoid emplacement in the Ghooli Dome and related aureole metamorphism by 90–140 Ma (Fig. 1).

### Classification as gold skarn deposits

Witt (2025) points out that the classification of Marvel Loch and Nevoria as gold skarn deposits is controversial.

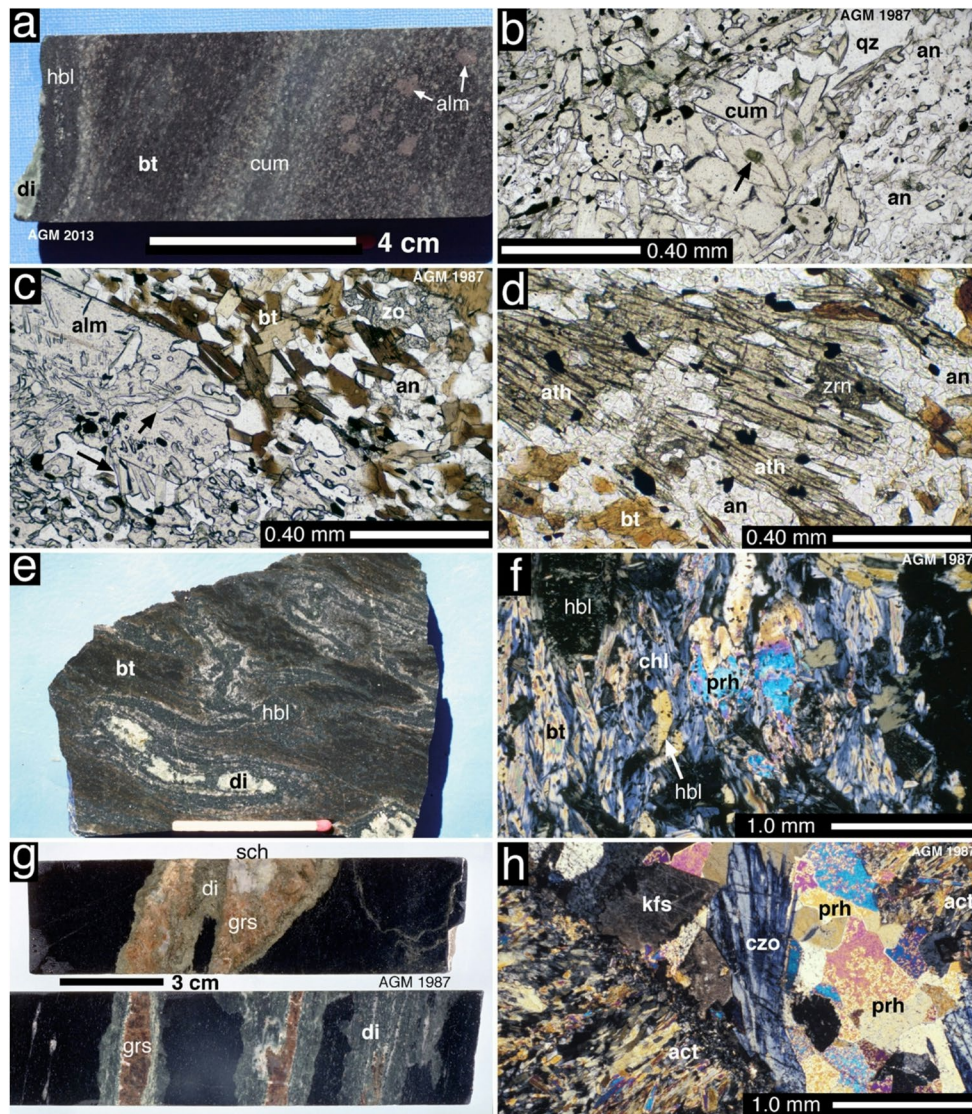


**Fig. 2** Nevoria gold skarn deposit, Southern Cross Belt, replacement in magnesian and tholeiitic amphibolite: Early prograde equilibrium assemblages in skarn at the footwall contact of BIF-1 (a-d), early zoned replacement with late assemblages (e-g), late retrograde skarn vein (h). (a) Diopside (di) zoned to hornblende (hbl) in contact with skarn composed of biotite (bt), cummingtonite (cum), anorthite, quartz, and almandine (alm). Drill hole NUG-12, 57.7 m. (b) Cummingtonite (cum) cored by metamorphic hornblende (arrow) in a matrix of anorthite (An96-97), quartz (qz), and ilmenite (opaque). NUG-12, 57.7 m, plane polarized light. (c) Almandine (alm) and cummingtonite (arrows) in mutual contact with biotite (bt), anorthite (an), and quartz. Retrograde zoisite (zo). NUG-12, 57.7 m, PPL. (d) Anthophyllite (ath) in anorthite (an), biotite (bt), quartz, Ti-magnetite

(opaque), and zircon (zrn). Drill hole NGM-9A, 189.0 m, 50 m west of NUG-12, PPL. (e) Diopside (di) and outer hornblende (hbl) + paragasite are zoned to biotite (bt) ± Fe-Mg chlorite. Nevoria East open pit, -55 m bench, the matchstick is 4 cm. (f) Outer zone hornblende (hbl) embayed by chlorite, in biotite (bt) + Fe-Mg chlorite (chl, blue birefringence) + prehnite (prh). Drill hole NUG-5, 36.9 m, crossed polars. (g) TOP: Zoned grossular-diopside (grs-di) vein, minor epidote, calcite, microcline, and scheelite (sch). NUG-12, 19.75 m. BOTTOM: Veins zoned from grossular (grs) ± epidote ± calcite to diopside (di) ± plagioclase, partly retrograded to prehnite + phengite. NUG-5, 49.0 m. (h) Late skarn vein filled with clinozoisite (czo) + prehnite (prh) + K-feldspar (kfs) + chlorite, bordered by selvages of actinolite (act). NUG-12, 7.20 m, crossed polars

Researchers from the University and the Geological Survey of Western Australia have promoted the metamorphic- orogenic fluid model for Archean gold deposits since the 1980s (Groves and Phillips 1987; Witt 1991; Witt et al. 1997, 2001, 2015; Groves et al. 1998, 2020; Ridley et al. 2000). In many of these publications, evidence for an intrusion-related model (Mueller 1991, 1997; Mueller et al.

1991, 2004) is not or rarely quoted, a tradition continued in Witt (2025). Apparently, he is not familiar with the terminology in classic reviews on skarn deposits (Einaudi et al. 1981; Einaudi 1982; Meinert et al. 2005). The occurrence of native gold in calc-silicates is necessary for the classification as skarn given that the gangue must be “spatially and temporally related to ore deposition”. In both the Marvel

Loch and Nevorioa skarns, gold was also deposited together with early and late sulfides in successive stages, contrary to the assertion in Witt (2025). Amongst the skarn minerals listed in Meinert et al. (2005; Table 1) are calc-silicates (anorthite, clinozoisite, prehnite) and Ca-poor silicates (almandine, cummingtonite) considered by many as metamorphic rather than hydrothermal. Biotite and K-feldspar, too, are not “unusual” (Witt 2025) but form outer potassic alteration up to 3 km wide around calcic gold skarns in the Hedley, British Columbia, and Battle Mountain districts, Nevada (Meinert 1998). Gedrite, cordierite, almandine, biotite and chlorite are part of the “skarnlike” high-T (600–550 °C) gangue associated with Au-Bi-Te ore in the Lucky Draw deposit, New South Wales, Australia (Sheppard et al. 1995; Meinert 1998).

## Gold skarns, I-type granites, and LCT pegmatites

Witt (2025) states that the link between high-T gold and granite intrusion requires further investigation, hardly surprising given the focus on metamorphic-orogenic fluid models. He also claims that the granite suite responsible for skarn and LCT pegmatite formation is poorly constrained. Again, his discussion is misleading. Structural evidence for syn-gold pegmatite emplacement at Marvel Loch (Mueller 1991) and at Corinthian (at  $2620 \pm 6$  Ma; Bloem et al. 1995) was not followed up, despite isotopic data supporting a granitic fluid source (Mueller et al. 1991). At Marvel Loch, crosscutting relations and native gold in pegmatite indicated multiple stages of emplacement, broadly coincident with skarn formation, which outlasted reverse-dextral movement in the contact-bound alteration zone (Mueller 1991). However, most skarn-associated pegmatites were interpreted as post-gold (Mueller and McNaughton 2000). This perception changed in 2004, when the Nevorioa gold skarn was dated at  $2635.7 \pm 1.2$  Ma, a concordant allanite-in-garnet U-Pb age within error of the zircon age ( $2634 \pm 4$  Ma) of the 500 m thick pegmatite-granite complex below the deposit (Mueller et al. 2004). The zoned Nevorioa intrusion and other pegmatitic granites associated with gold skarns were then identified as fractionated members of a post-orogenic suite of I-type biotite granites emplaced into continental crust at 2665–2615 Ma, research expanded on in Mueller (2025). Doublie et al. (2014; their Fig. 1) report pegmatite ages (2634–2620 Ma) for four gold deposits located in the metamorphic aureole of the Ghooli Dome. They link mineralization to low-Ca granite-pegmatite emplacement at 2640–2620 Ma, in agreement with Mueller et al. (2004). The classification into high- and low-Ca granites is not used in Mueller (2025), because the I-type/S-type

and magnetite- versus ilmenite-series classifications provide more reliable links to ore deposit formation (e.g. Ishihara 1981). Even less helpful are local names such as the Woolgangie or Bali suites. Spodumene-bearing LCT pegmatites were emplaced at 2650–2620 Ma (Greenbushes:  $2631 + 4/-9$  Ma) into all terranes of the Yilgarn Craton at about 15 km depth ( $400 \pm 100$  MPa; Wells et al. 2025). LCT pegmatites and high-T gold skarn deposits such as Marvel Loch (400 MPa; Mueller et al. 1991) and Nevorioa (300–400 MPa; Mueller et al. 2004) formed at the same time and in the same batholithic environment. Li-Cs-Ta pegmatites are not solely an expression of crustal depth (Witt 2025) but are the most fractionated members of a fertile granite suite (Cerny and Meintzer 1988; Cerny et al. 2005), which must be identified. Less fractionated, peraluminous, ilmenite-series (?) pegmatitic granites like the Nevorioa pluton are members of the same I-type suite (Mueller 2025). Given the spatial coincidence, mining companies should explore for both gold and lithium in lease areas where garnet-muscovite pegmatites are exposed (Mueller 2025). In the Nevorioa granite, primary inclusions in quartz trapped a low-density, 3-phase H<sub>2</sub>O-CO<sub>2</sub> fluid with variable liquid-vapor ratios (SG Hagemann, personal communication 2004), similar to the low-salinity (0.1–10 wt% NaCl<sub>eq</sub>) H<sub>2</sub>O-CO<sub>2</sub>±CH<sub>4</sub> fluid trapped in grossular-diopside veins (Fig. 2g) and in the gold skarn (Fan et al. 2000). Thus, the Nevorioa deposit represents an excellent opportunity to resolve the uncertainty about the role of magmatic fluids in Archean gold skarns.

**Funding** Open Access funding enabled and organized by Projekt DEAL. No funding was received.

## Declarations

**Conflict of interest** There are no conflicts of interest.

**Open Access** This article is licensed under a Creative Commons Attribution 4.0 International License, which permits use, sharing, adaptation, distribution and reproduction in any medium or format, as long as you give appropriate credit to the original author(s) and the source, provide a link to the Creative Commons licence, and indicate if changes were made. The images or other third party material in this article are included in the article's Creative Commons licence, unless indicated otherwise in a credit line to the material. If material is not included in the article's Creative Commons licence and your intended use is not permitted by statutory regulation or exceeds the permitted use, you will need to obtain permission directly from the copyright holder. To view a copy of this licence, visit <http://creativecommons.org/licenses/by/4.0/>.

## References

- Ahmat AL (1986) Metamorphic patterns in the greenstone belts of the Southern Cross Province, Western Australia. Geol Surv West Australia, Prof Paper 19:1–21

- Bloem EJM, McNaughton NJ, Groves DI, Ridley JR (1995) An indirect lead isotope age determination of gold mineralization at the Corinthia Mine, Yilgarn Block, Western Australia. *Aust J Earth Sci* 42:447–451
- Cerný P, Meintzer RE (1988) Fertile granites in the Archean and Proterozoic fields of rare-element pegmatites: crustal environment, geochemistry and petrogenetic relationships. In: Taylor RP, Strong DF (eds) Recent advances in the geology of granite-related mineral deposits. *Can Inst Min Metall Special Volume* 39:170–207
- Cerný P, Blevin PL, Cuney M, London D (2005) Granite-related ore deposits. *Econ Geol* 100th Anniversary Vol, 337–370
- Dalstra HJ, Bloem EJM, Ridley JR, Groves DI (1998) Diapirism synchronous with regional deformation and gold mineralization, a new concept for granitoid emplacement in the Southern Cross Province, Western Australia. *Geol Mijnbouw* 76:321–338
- Doublier MP, Thebaud N, Wingate MTD, Romano SS, Kirkland CL, Gessner K, Mole DR, Evans N (2014) Structure and timing of Neoproterozoic gold mineralization in the Southern Cross district (Yilgarn Craton, Western Australia) suggest leading role of late low-Ca I-type granite intrusions. *J Struct Geol* 67:205–221
- Einaudi MT (1982) Description of skarns associated with porphyry copper plutons. In: Tittle SR (ed) Advances in geology of the porphyry copper deposits, southwestern North America. *Univ Arizona, Tucson*, pp 139–183
- Einaudi MT, Meinert LD, Newberry RJ (1981) Skarn deposits. *Econ Geol* 75th Anniversary Vol, 317–391
- Fan HR, Groves DI, Mikucki EJ, McNaughton NJ (2000) Contrasting fluid types at the Nevoia gold deposit in the Southern Cross greenstone belt, Western Australia: implications of auriferous fluids depositing ores within an Archean banded iron-formation. *Econ Geol* 95:1527–1536
- Groves DI, Phillips GN (1987) The genesis and tectonic control on Archean gold deposits of the Western Australian shield: a metamorphic-replacement model. *Ore Geol Rev* 2:287–322
- Groves DI, Goldfarb RJ, Gebre-Mariam M, Hagemann SG, Robert F (1998) Orogenic gold deposits: a proposed classification in the context of their crustal distribution and relationship to other deposit types. *Ore Geol Rev* 13:7–27
- Groves DI, Santosh M, Deng J, Wang Q, Yang L, Zhang L (2020) A holistic model for the origin of orogenic gold deposits and its implications for exploration. *Miner Deposita* 55:275–292
- Ishihara S (1981) The granitoid series and mineralization. *Econ Geol* 75th Anniversary Vol , 458–484
- Libby JW, Groves DI, Vearncombe JR (1991) The nature and tectonic significance of the crustal-scale Koolyanobbing shear zone, Yilgarn craton, Western Australia. *Aust J Earth Sci* 38:229–245
- Liou JG, Kim HS, Maruyama S (1983) Prehnite-epidote equilibria and their petrologic applications. *J Petrol* 24:321–342
- Lu Y, Wingate MTD, Kirkland CL (2017) 199021: quartz-muscovite schist, Copperhead mine. *Geol Surv West Australia Geochronology Record* 1422, 4 pp
- Meinert LD (1998) A review of skarns that contain gold. In: Lentz DR (ed) Mineralized intrusion-related skarn systems. *Min Ass Canada, Short Course* 26: 359–414
- Meinert LD, Dipple GM, Nicolescu S (2005) World skarn deposits. *Economic Geology* 100th Anniversary Vol, 299–336
- Mueller AG (1991) The Savage Lode magnesian skarn in the Marvel Loch gold-silver mine, Southern Cross greenstone belt, Western Australia: Part I. Structural setting, petrography and geochemistry. *Can J Earth Sci* 28:659–685. <https://doi.org/10.1139/e91-059>
- Mueller AG (1997) The Nevoia gold skarn deposit in Archean iron-formation, Southern Cross greenstone belt, Western Australia: I. Tectonic setting, petrography, and classification. *Econ Geol* 92:181–209. <https://doi.org/10.2113/gsecongeo.92.2.181>
- Mueller AG (2025) Granite-pegmatite-related gold skarns and associated Li-Cs-Ta pegmatites in the Archean Yilgarn Craton, Western Australia. *Miner Deposita* 60:835–867
- Mueller AG, McNaughton NJ (2000) U-Pb ages constraining batholith emplacement, contact metamorphism, and the formation of gold and W-Mo skarns in the Southern Cross area, Yilgarn craton, Western Australia. *Econ Geol* 95:1231–1257. <https://doi.org/10.2113/gsecongeo.95.6.1231>
- Mueller AG, Groves DI, Delor CP (1991) The Savage Lode magnesian skarn in the Marvel Loch gold-silver mine, Southern Cross greenstone belt, Western Australia: Part II. Pressure-temperature estimates and constraints on fluid sources. *Can J Earth Sci* 28:686–705. <https://doi.org/10.1139/e91-060>
- Mueller AG, Nemchin AA, Frei R (2004) The Nevoia gold skarn deposit, Southern Cross greenstone belt, Western Australia: II. Pressure-temperature-time path and relationship to postorogenic granites. *Econ Geol* 99:453–478. <https://doi.org/10.2113/gsecongeo99.3.453>
- Qiu YM, McNaughton NJ, Groves DI, Dalstra HJ (1999) Ages of internal granitoids in the Southern Cross region, Yilgarn Craton, Western Australia, and their crustal evolution and tectonic implications. *Aust J Earth Sci* 46:971–981
- Ridley JR, Groves DI, Knight JT (2000) Gold deposits in amphibolite and granulite facies terrains of the Archean Yilgarn craton, Western Australia: evidence and implications of syn-metamorphic mineralisation. In: Marshall B, Vokes FM (eds) Metamorphic and metamorphogenic ore deposits. *Rev Econ Geol* 11: 265–290
- Sheppard S, Walshe JL, Pooley JD (1995) Noncarbonate, skarnlike Au-Bi-Te mineralization, Lucky Draw, New South Wales, Australia. *Econ Geol* 90:1553–1569
- Thebaud N, Mole DM, Wingate MTD, Kirkland CL, Doublier MP (2013a) 205916: metasyenogranite, Withers Find road. *Geol Surv West Australia, Geochronology Record* 1121, 5 pp
- Thebaud N, Wingate MTD, Kirkland CL, Doublier MP (2013b) 205912: granodiorite gneiss, Lake Julia. *Geol Surv West Australia Geochronology Record* 1114 , 5 pp
- Wells MA, Aylmore MG, McInnes BIA, Rickard WDA, Rankenburg K (2025) Mineral-textural characteristics of lithium pegmatite ores of Western Australia. *Econ Geol* 120:1287–1310
- Witt WK (1991) Regional metamorphic controls on alteration associated with gold mineralization in the Eastern Goldfields province, Western Australia: implications for the timing and origin of Archean lode-gold deposits. *Geology* 19:982–985
- Witt WK (2025) Discussion on "Granite-pegmatite-related gold skarns and associated Li-Cs-Ta pegmatites in the Archean Yilgarn Craton " by Mueller (2025). *Mineralium Deposita*. <https://doi.org/10.1007/s00126-025-01416-1>
- Witt WK, Knight JT, Mikucki EJ (1997) A synmetamorphic lateral fluid flow model for gold mineralization in the Archean Southern Kalgoorlie and Norseman terranes, Western Australia. *Econ Geol* 92:407–437
- Witt WK, Drabble M, Bodycoat FM (2001) Yilgarn Star gold deposit, Southern Cross greenstone belt, Western Australia: geological setting and characteristics of an amphibolite-facies orogenic gold deposit. *Geol Surv West Aust Rec* 2001/17:45–62
- Witt WK, Ford A, Hanrahan B (2015) District-scale targeting for gold in the Yilgarn craton: Part 2 of the Yilgarn gold exploration targeting atlas. *Geol Surv West Aust Rep* 132 , 276 pp